RC23206 (W0405-047) May 10, 2004
Materials Science

IBM Research Report

Small Angle X-ray Scattering Metrology for Sidewall Angle and Cross Section of Nanometer Scale Gratings

Tengjiao Hu, Ronald L. Jones, Wen-li Wu, Eric K. Lin
Polymers Division
MSEL
National Institute of Standards and Technology
Gaithersburg, MD 20899-8541

Qinghuang Lin
IBM Research Division
Thomas J. Watson Research Center
P.O. Box 218
Yorktown Heights, NY 10598

John Quintana
DND-CAT
Advanced Photon Source
Argonne National Laboratory
Argonne, IL 60439

Research Division
Almaden - Austin - Beijing - Haifa - India - T. J. Watson - Tokyo - Zurich

Small angle X-ray scattering metrology for sidewall angle and cross section of nanometer scale gratings[†]

Tengjiao Hu, Ronald L. Jones, Wen-li Wu,[*] Eric K. Lin
Polymers Division, MSEL, National Institute of Standards and Technology, Gaithersburg, Maryland 20899-8541
Qinghuang Lin
IBM Thomas J. Watson Research Center, P.O. Box 218, Yorktown Heights, New York 10598
John Quintana
DND-CAT, Advanced Photon Source, Argonne National Laboratory, Argonne, Illinois 60439

Abstract

Fabrication of nano-structures requires non-destructive metrologies capable of not only measuring the pattern size but also the pattern shape profile. This demand will become more stringent as the feature size shrinks to tens of nanometers, where tolerances of pattern shape will be measured in nanometers. Previously we have demonstrated that a small angle X-ray scattering (SAXS) based technique has the capability of characterizing the average pitch size and pattern width to sub-nanometer precision. In this study, we further develop a protocol to extract the cross-section information of grating patterns, such as the average sidewall angle and pattern height. The appropriate reciprocal space map is probed by measuring diffraction peak intensities when the sample is rotated around the axis perpendicular to its grating direction. As an additional part of the sidewall angle determination, rotation of the sample also allows a precise determination of the pattern height.

---

[*] To whom all correspondence should be addressed. Email: wen-li.wu@nist.gov

Introduction

Nanometer scale control of lithographic pattern quality is required as the semiconductor industry moves to mass production of sub-100 nm devices.[1] Specifically, metrologies capable of providing information on the cross section of patterns are a critical component to the development of practical nanofabrication methods. Scanning electron microscopy (SEM) has been the mainstay inspection metrology in lithography.[2,3] Other methods, such as atomic force microscopy (AFM) and light scatterometry,[4-6] have also been proposed as alternative metrologies to measure pattern quality. Unfortunately, all of these metrologies face challenges as device features continue to shrink to the scale of tens of nanometers. For example, these three metrologies are expected to be less effective in measuring dense, high aspect ratio, as well as buried features, with decreasing feature size.[7-9] As a result, the development of a metrology for measuring a line-edge roughness on the scale of only a few nanometers and a sidewall angle close to zero degrees is listed as one of the five major inspection metrology challenges in the recently revised "International Technology Roadmap for Semiconductors" (ITRS).[10]

Recently we have been developing a new technique based on small angle X-ray scattering (SAXS) as an alternative to characterize patterns with a critical dimension (CD) on the scale of nanometers.[11-13] Critical Dimension-Small Angle X-ray Scattering (CD-SAXS) has several potential advantages over other existing inspection metrologies such as increased sensitivity to smaller features, a capability of measuring dense high aspect ratio patterns as well as buried patterns. Earlier results have demonstrated that CD-SAXS can provide a fast and accurate measurement of the average pitch size and pattern

width of testing grating patterns from the position and relative scattering intensity of diffraction peaks. However, elements of the measured data suggest that there is more detail that can be extracted on pattern shape and quality using refined methods of measurement. As an example, the peak intensity along the diffraction axis decays more rapidly than expected from a simple rectangular model for the pattern profile.[13] A more rapid decay has many potential origins such as a random deviation in pitch size, line-edge roughness (LER), and a non-rectangular grating shape profile.[14]

In this paper, we describe a general methodology for probing the cross section of patterns. We then apply the methodology to extract the average sidewall angle of photoresist gratings prepared by optical lithography. In this particular case, a trapezoid is used to model the cross section and the average sidewall angle is extracted. With the average pattern height and width, the entire cross section of the pattern is therefore provided. The results are compared to the cross sectional SEM images of the patterns.

Experiment

The samples consist of a series of equally spaced parallel lines prepared directly on a 200 mm in diameter single crystal silicon wafer. 248 nm optical lithography was used to produce this grating structure with a nominal 150 nm line width and a line space ratio of 1:1. The samples discussed here are labeled as Sample A and B, imaged with a depth of focus deviation of 0.4 μm and 0.2 μm, respectively. Cross sectional SEM images (Figure 1) indicate that the cross section of the patterns is approximately trapezoidal with a noticeable difference between the sidewall angles for these two samples.

The CD-SAXS measurements were performed at the 5ID-DND beamline of the Advanced Photon Source (Argonne National Laboratory) using a 2D CCD detector. The

X-ray wavelength was set to 0.729 Å using a double monochromator. At this wavelength, there is still ~20% transmission of the incident beam through the industrial standard silicon wafers. The beam was collimated by two sets of slits to a size of 120×180 μm^2 measured at sample position. In the present experiment, a smaller beam size is not necessary. However, a further decrease of beam size to characterize industrial test structures on the order of 50×50 μm^2 is feasible as demonstrated in our earlier experiment. One ion chamber was used to monitor the incident beam intensity and it was found that there was no obvious intensity fluctuation or drift of the incident beam during the measurement. The sample was rotated around the Y-axis, as defined in Figure 2, from nominal –20° to 20° in a step size of (1 ± 0.05)°. The 2D detector was placed at (700 ± 1) cm from the sample. It has a resolution of (78.75 ± 0.01) μm per pixel and 2048 pixels in each direction. In contrast to our prior experiments, the air scattering is greatly reduced here with the use of an evacuated sample chamber, whose pressure was on the order of 10^{-3} Torr.

In order to make a consistent comparison between scattering at different rotation angle, a correction of the beam path length is necessary due to the large attenuation of the X-ray beam by the silicon substrate. As we rotate the sample, the effective transmission path changes as d/cosφ, where d is the thickness of the silicon substrate (~1 mm) if we neglect the pattern height (~0.3 μm).

Results and discussion

The intensity contours in Figure 3 represent the form factor of an isolated trapezoid in Fourier space, which is taken as the average cross section of the grating patterns.

Specifically, the bevel edges of the patterns result in a series of scattering streaks with an angle of $\pm\beta$ from the q_x axis in the q_x-q_z plane, as indicated by the eye-guiding lines in this figure. Interference of multiple trapezoids results in vertical ridges with a spacing of $2\pi/D$, where D is the pitch of the grating. The complete Fourier transform is therefore described as a set of vertical ridges, whose positions are defined by the reciprocal lattice of the grating, and whose intensities are defined by the form factor of the trapezoid.

The determination of the pattern cross section therefore requires a measurement of scattered intensity in the q_x-q_z plane. In the small angle X-ray scattering configuration reported previously, the beam is always normal to the substrate and primarily probes the scattering in q_x-q_y plane, with a limited variation in q_z as scattering angle increases. There are several potential approaches to probe the q_z dependence of the scattering intensity. One is to measure the scattering at a very large scattering angle, where the contribution of q_z to the total wave vector cannot be neglected. Another is to vary the X-ray wavelength, which will push the surface of the Ewald sphere forward or backward (i.e., probing different q_z's). However, the diffraction peak intensity decays very fast as the scattering angle increases. In addition, a variation of the X-ray wavelength is not always convenient and practical. A third method of probing $I(q_z)$ is achieved by measuring the small angle scattering of samples at different sample rotation angles, φ, as indicated in Figure 2. Experimentally, diffraction peaks occur at the intersections between the reciprocal lattice and the Ewald sphere in the q_x-q_y plane. By collecting data over a range of φ, the reciprocal space map of the sample is rotated relative to the Ewald sphere, and the positions of the diffraction peaks can be transformed back to the original q_x-q_z plane. In this way, the theoretical map of Figure 3 can be obtained. The advantage of this approach

is the use of the small q_x regime, providing relatively high signal-to-noise data over alternative methods.

Based on this methodology, the intensity of a given diffraction peak as a function of sample rotation angle, φ, traces a vertical line in Figure 3 (i.e. approximately constant q_x). The direct correspondence of the angle between the intensity streaks in Figure 3 and the sidewall angle, β, points to a simple and intuitive way to extract the average sidewall angle from scattering data in the q_x-q_z plane. It further suggests scattering intensity of all diffraction orders reaches a maximum as the rotation angle φ approaches β.

Figure 4 shows the rotation angle dependence of the peak intensity for the 2^{nd} order diffraction peak. Due to a lack of precise sample alignment in the current experimental system, the midpoint between the two primary peaks was chosen as the origin (i.e. φ=0) on the abscissa. However, this step is not necessary if high precision sample alignment equipment becomes available for future work. The theoretically calculated peak intensity with only one varying parameter (the sidewall angle of the pattern) shows a qualitative agreement with the experimental data. The fitting gives a sidewall angle of ≈ 5.0º. A good agreement between the experimental values and the calculated ones was also observed for the second maximum in Figure 4. In contrast to the complicated modeling in light scatterometry, the average sidewall angle of the sample can be estimated by locating the rotation angle φ where every diffraction peak reaches its global maximum without any modeling or fitting. The corresponding results from Sample B indicate that the sidewall angle is ≈ 3.0º. This agrees qualitatively with the SEM results given in Figure 1 taken with a tilt angle of 30º.

Also noticed in Figure 4 the observed peak intensity went through multiple maxima and minima. Figure 5 provides a set of calculated results of the peak intensity of the 5^{th}, 6^{th} and 7^{th} order diffraction peaks over a range of φ for a sidewall angle of 5°. Regardless of the peak order all intensities reach their global maximum at the same rotation angle φ. Higher order peaks reach the next maximum earlier than lower orders. The reason can be readily found in Figure 3 where the line representing the Ewald sphere will touch point 3' at lower φ than that for point 1'. While the type of approach shown in Figure 4 can provide an estimation of the sidewall angle, one can enhance the precision by analyzing the entire data set collectively. Data from Sample A is used to illustrate the new and collective approach for determining sidewall angle. The positions of the maxima and minima of all the observed peaks in terms of their coordinates on the $q_x - q_z$ plane are now plotted in Figure 6. We note that the series of diffraction peaks are indeed reminiscent of the form predicted theoretically in Figure 3. Most noticeable is that the extrapolations of both branches of first maximum lines go through the origin of the q_x–q_z plane. We should mention that in this representation of experimental data, the lines within each positive and negative branch are not perfectly parallel. This is especially obvious for the data points of the first minima. This kind of deviation may have several origins. One possibility is deviation of the cross section of the pattern from a trapezoid. The existence of streaks in Figure 6, however, suggests that the trapezoid model is at the least a good approximation of the average cross section. Uncertainty in sample alignment with respect to the incident beam and also the uncertainty between the rotation axis and y-axis are other possibilities. This shortfall can be overcome with a high precision alignment tool. In addition, compared to the intensity near the maxima, the intensity

around the minima is not distinguishably higher than the background scattering. This causes a significant uncertainty in determining the actual position of the minima. Therefore, only data points of peak maxima were used in this work for sidewall angle determination. Using the linear fits of the major maxima, we find that the effective sidewall angle has a value of $(5.7 \pm 0.2)^{o}$ for Sample A.

In the above analysis only the positions of the maxima and minima are plotted and analyzed. The result clearly demonstrates a capacity for accurate determination of the average cross section of patterns. It is likely that more information on the cross sectional shape such as higher order deviations from a trapezoid can be deduced through careful modeling efforts to account for all the observed peak intensities on the q_x–q_z plane.

In our previous publication we proposed to obtain the pattern height from the absolute intensity of diffraction peaks provided that the scattering cross section of the grating material is a given. Since experimental data are now available over a wide q_z range as given in Figure 6, we can determine the pattern height from the intercept of a line connecting the secondary maxima (i.e. 1', 2', 3', etc. in Figure 3). The height, H, of the trapezoid is simply related to the intercept via $2\pi/\Delta q_z$, where Δq_z is the value of the intercept of the line, as given in Figure 6. For Sample A, the height is ≈318 nm, which is consistent with the result from the fitting of the relative peak intensity. This provides a preferable way to obtain pattern height since there is no need for a prior knowledge of scattering cross section of the grating materials and the scattering intensity observed does not need to be reduced to its absolute scale.

Summary

Inspection of the cross sectional profile for lithographic patterns has been listed as one of the five major challenges in the recent revised version of ITRS. Based on our previous work on CD-SAXS metrology, we further developed a new protocol to determine sidewall angle of patterns by collecting scattering data at various rotation angles. For illustration, a simple trapezoidal cross section was chosen to model the sample scattering. Data from two testing samples were collected and analyzed in terms of the positions of the intensity maxima and minima of the diffraction peaks as we rotated the sample. The sidewall angle determined is qualitatively in agreement with what shown in SEM micrographs. In addition this method also provides a convenient measurement of pattern height.

Acknowledgement

This work was funded in part by the DARPA Advanced Lithography Program under contract N66001-00-C-8803. Additional funding was provided by the NIST Office of Microelectronic Programs. R. L. J. is supported by a NIST National Research Council postdoctoral fellowship. Steve Weigand and Denis Keane (DND-CAT, APS) provided valuable technical support.

References

1 H. M. Marchman, J. E. Griffith, J. Z. Y. Guo, J. Frackoviak, G. K. Celler, *J. Vac. Sci. Technol. B*, 1994, **12(6)**, 3585.

2 Li-Jui Chen, Shang-Wei Lin, Tsai-Sheng Gau, Burn J. Lin, *SPIE Proceedings*, 2003, **5038**, 166.

3 Eric Solecky, Chas Archie, Jason Mayer, Roger Cornell, Ofer Adan, *SPIE Proceedings*, 2003, **5038**, 518.

4 Ronald Dixson, Angela Guerry, Marylyn Bennett, Theodore Vorburger, Ben Bunday, *SPIE Proceedings*, 2003, **5038**,150.

5 Eytan Barouch, Stephen L. Knodle, *SPIE Proceedings*, 2003, **5038**, 559.

6 Li-Jui Chen, Chih-Ming Ke, Shinn-Sheng Yu, Tsai-Sheng Gau, Pei-Hung Chen, Yao-Ching Ku, Burn J. Lin, *SPIE Proceedings*, 2003, **5038**, 568.

7 A. V. Nikitin, A. Sicignano, D. Y. Yeremin, M. Sandy, T. Goldburt, *SPIE Proceedings*, 2003, **5038**, 651.

8 Kouji Kimura, Kazuo Abe, yasuko Tsuruga, Hitoshi, Nobuo Kochi, Hirotami Koike, Yuichiro Yamazaki, *SPIE Proceedings*, 2003, **5038**, 1089.

9 B. C. Park, J. Kang, K. Y. Jung, W. Y. Song, B.-h. O, T. B. Eom, *SPIE Proceedings*, 2003, **5038**, 935.

10 *International Technology Roadmap for Semiconductors*, http://public.itrs.net/Files/2003ITRS/Home2003.htm, 2003.

11 Wen-li Wu, Eric K. Lin, Qinghuang Lin, Marie Angelopolous, *J. Appl. Phys.*, 2000, **88(12)**, 7298.

12 Ronald L. Jones, Tengjiao Hu, Eric K. Lin, Wen-li Wu, Rainer Kolb, Diego M. Casa, Patrick J. Bolton, George G. Barclay, *Appl. Phys. Lett.*, 2003, **83(19)**, 4059.

13 Tengjiao Hu, Ronald L. Jones, Wen-li Wu, Christopher Soles, Eric K. Lin, Arpan Mahorowala, Diego M. Casa, *Polymer Preprints,* 2003, **44(2)**, 541.

14 A. Guinier, *X-ray diffraction in crystals, imperfect crystals, and amorphous bodies*, Dover Publications, Inc., New York, 1994.

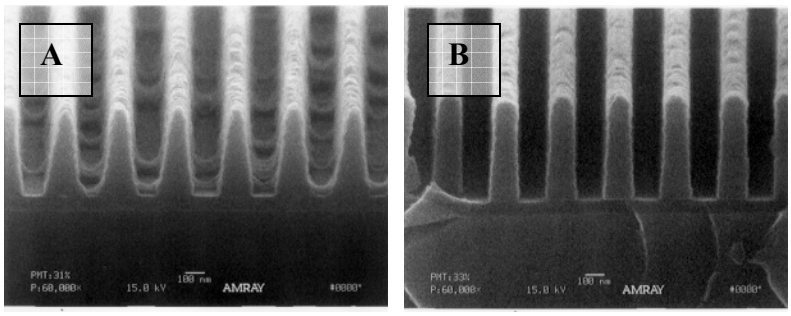

Figure 1 SEM micrograph of the grating patterns with +0.4 and +0.2 μm of focus depth deviation from optimal image conditions.

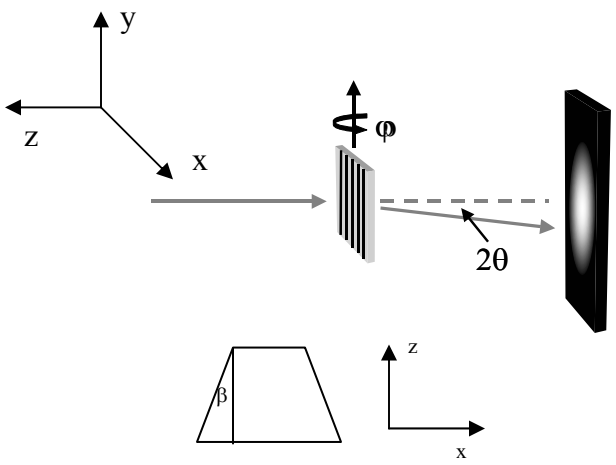

Figure 2 Schematic of the small angle X-ray scattering geometry illustrating the scattering angle 2θ, the sample rotation angle φ and sample sidewall angle β.

Figure 3 Contour plot of the calculated scattering intensity for a trapezoidal cross section on the q_x–q_z plane. The lattice points of an equally spaced grating are given as the set of vertical lines. The Ewald sphere is depicted as a straight line at a rotation angle φ. The dimensions of the trapezoid used in this calculation are; height = 2000 Å, width at middle = 1200 Å, sidewall angle β = 63.43°, repeat of the grating = 2000 Å.

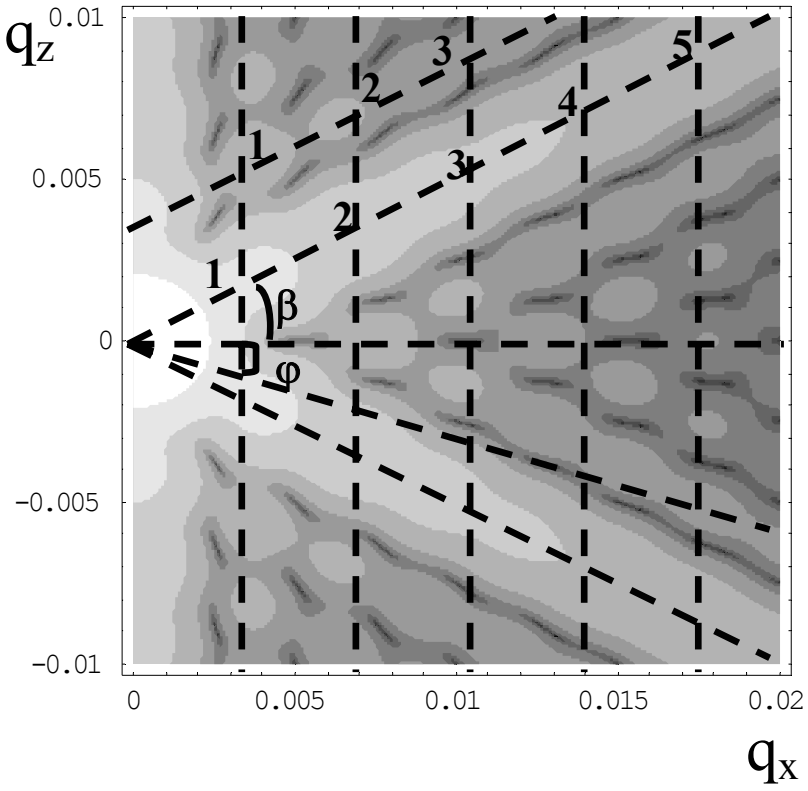

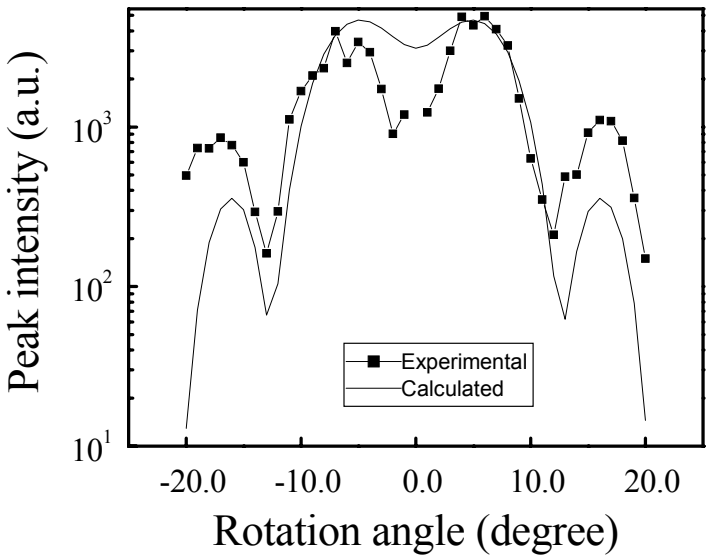

Figure 4 Experimental data of Sample A and the corresponding theoretically calculated peak intensities of the 5th order diffraction at different rotation angles.

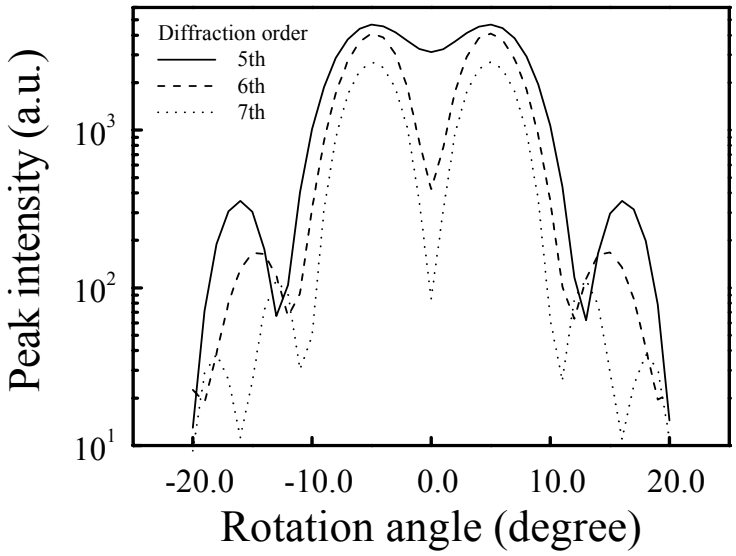

Figure 5 Calculated rotation angle dependence of the diffraction peak intensities at three different diffraction orders. The sidewall angle in the model is 5.0º.

Figure 6 Diffraction peak positions of the maxima and minima intensities of Sample A in the q_x–q_z plane. Lines are drawn to connect the observed maxima.